Acta Cryst. (1987). B43, 76-83

Structural Studies by Electron and X-ray Diffraction of the Disordered Phases II': $(Sn_{1-x}Tb_x)Tb_4Rh_6Sn_{18}$ and $(Sn_{1-x}Dy_x)Dy_4Os_6Sn_{18}$

BY S. MIRAGLIA,* J. L. HODEAU, F. DE BERGEVIN AND M. MAREZIO

Laboratoire de Cristallographie, CNRS, associé à l'Université Scientifique et Médicale de Grenoble, 166 X, 38042 Grenoble CEDEX, France

AND G. P. ESPINOSA

AT&T Bell Laboratories, Murray Hill, New Jersey 07974, *USA*

(*Received* 21 *March* 1986; *accepted* 4 *September* 1986)

Abstract

$(Sn_{1-x}Tb_x)Tb_4Rh_6Sn_{18}$ and $(Sn_{1-x}Dy_x)Dy_4Os_6Sn_{18}$ belong to a large stannide series where there exist two chemical formulae: $SnM_3M'_4Sn_{12}$ (phase I and I') and $SnM_4M'_6Sn_{18}$ (phase II and II'), and four structures: I, I', II and II'. That of phase II' appeared to be cubic ($a \simeq 13{\cdot}7$ Å and space group $Fm3m$) while the structure of phase II is tetragonal ($a \simeq 13{\cdot}7$, $c \simeq 27{\cdot}4$ Å and space group $I4_1/acd$). Phase II' of the M = Tb, M' = Rh stannide was found to be a disordered microtwinned phase II. The disorder concerned the Tb(2) and Sn(2) sublattices of formula: $[Sn(1)_{1-x}Tb_x]Tb(2)_4Rh_6Sn(2)_4Sn(3)_{12}Sn(4)_2$. This qualitative model is based on the observation of weak intermittent diffuse streaks and on refinements of the average cubic structure, carried out by taking into account only Bragg reflections. The results proved that phases II and II' had related structures and the same chemical formulae. The complete reciprocal lattice (Bragg + diffuse scattering) was obtained by electron diffraction for the M = Dy, M' = Os stannide. The diffuse streaks are lines parallel to the {100} cubic ($a_{II'} \times a_{II'} \times a_{II'}$) directions and going through the F-centering-forbidden nodes. The three sets of lines are related by the cubic threefold $[111]_{II'}$ axis. It is observed that phase II structure contains eight-atom [4Sn(2), 4M(2)] blocks which can have two orientations (here called A and B). It can be surmised that the same blocks exist in phase II', but in a partially disordered arrangement. Two equivalent descriptions of this arrangement are given: (1) ordered (100) planes of A and B blocks are stacked at random and the threefold-axis-twinned individuals give rise to three sets of streaks; (2) the A and B blocks form an f.c.c. lattice which is comprised of tetrahedra formed of nearest neighbours; it is shown that when each cluster contains two A and two B blocks, diffuse scattering condenses into the observed streaks. Crystal data for $(Sn_{1-x}Tb_x)Tb_4Rh_6Sn_{18}$, x = 1: $M_r = 3548{\cdot}5$, disordered microtwinned tetragonal, $I4_1/acd$, $a = 13{\cdot}772\,(2)$ Å, $c = 2a$, $V = 5224{\cdot}2$ Å^3, Z = 8, $D_x = 9{\cdot}02$ g cm^{-3}, Ag $K\alpha$, graphite monochromator, $\mu = 175{\cdot}9$ cm^{-1}, $F(000) = 11\,960$, T = ambient.

Introduction

The $(Sn_{1-x}Tb_x)Tb_4Rh_6Sn_{18}$ and $(Sn_{1-x}Dy_x)Dy_4Os_6Sn_{18}$ compounds belong to a large series of intermetallic stannides with formulae $SnM_3M'_4Sn_{12}$ or $(Sn_{1-x}M_x)M_4M'_6Sn_{18}$, with M = RE (rare earth), Y, Sc, Ca, Sr, Th and M' = Rh, Ru, Ir, Os, Co. These stannides exhibit magnetic and/or superconducting properties; for example, reentrant superconductivity ($T_c \simeq 1$, $T_m \simeq 0{\cdot}5$ K) was found in the compound with M = Er and M' = Rh (Remeika *et al.*, 1980). Four different phases have been reported in this system, namely I, I', II and II', whose structures may be described by means of three-dimensional networks of corner-sharing $M'Sn_6$ trigonal prisms. The way the prisms are joined together leads either to phase I and I' compounds with the chemical formula $SnM_3M'_4Sn_{12}$ or to phase II and II' compounds with the chemical formula $(Sn_{1-x}M_x)M_4M'_6Sn_{18}$. In some previous publications phase II' was called phase III. Phase I is cubic (space group $Pm3n$, $a_I \simeq 9{\cdot}7$ Å). In this structure the corner-sharing trigonal-prism network generates icosahedral and cuboctahedral sites occupied by the Sn(1) and M atoms. These latter atoms form a sublattice having the arrangement of an $A15$ structure (Vandenberg, 1980; Hodeau, Chenavas, Marezio & Remeika, 1980). Phase I' compounds have a slightly distorted phase I structure; its symmetry is either cubic with $a_{I'} = 2a_I$ or tetragonal with $a_{I'} = a_I 2^{1/2}$ and $c_{I'} = a_I$ (Hodeau, Marezio, Remeika & Chen, 1982; Miraglia, Hodeau, Marezio, Laviron, Ghedira & Espinosa, 1986). Phase II is tetragonal (space group $I4_1/acd$, $a_{II} \simeq 13{\cdot}7$, $c_{II} \simeq 2a_{II}$). Its chemical formula corresponds

* Present address: KFK, ITP Postfach 3640, D-7500 Karlsruhe, Federal Republic of Germany.

0108-7681/87/010076-08$01.50

to $[Sn(1)_{1-x}M(1)_x]M(2)_4M'_6Sn(2)_4Sn(3)_{12}Sn(4)_2$ (Hodeau, Marezio & Remeika, 1984). The crystal structure is rather complex, but it can be described as the result of interpenetrated sublattices. The Sn(2) and Sn(3) atoms form a three-dimensional network of corner-sharing trigonal prisms whose centers are occupied by the M' atoms. The Sn(4) atoms are only bonded to $M(2)$ atoms and do not participate in the formation of the trigonal-prism network. The $[Sn(1)_{1-x}M(1)_x]M(2)_4$ sublattice is comprised of two interpenetrating f.c.c. lattices: one formed by disordered Sn(1) and $M(1)$ atoms and the other by $M(2)_4$ tetrahedra.

Phase II′ appears to be cubic ($a_{II'} = a_{II}$); however, preliminary studies on the M = Tb, M' = Rh compound revealed on the precession photographs the presence of intermittent diffuse streaks exactly where the spots responsible for doubling the c axis appeared on the precession photographs of phase II. This prompted the authors to surmise that the tetragonality of phase II existed also in phase II′ but only in a short-range fashion (Chenavas, Hodeau, Collomb, Marezio, Remeika & Vandenberg, 1981). Since the observed diffuse streaks could not be taken into account in the structural refinements, no model could be proposed for the phase II′ compounds, and average structures were obtained (Vandenberg, 1980; Chenavas *et al.*, 1981). Electron diffraction can be a suitable tool to determine the reciprocal lattice including the diffuse scattering. A study of the M = Dy, M' = Os compound was undertaken by TEM (transmission electron microscopy) and new structural refinements based on X-ray data were carried out for the M = Tb, M' = Rh stannide. This allowed us to reconstruct the reciprocal lattice completely and to propose a model of disorder which takes into account the Bragg reflections as well as the diffuse scattering.

X-ray measurements

All the single crystals were grown by dissolving the starting elements in evacuated fused silica tubes at ~1320 K, followed by a cooling rate of 5 K h^{-1} to 820 K. More details about the crystal-growth process are reported elsewhere (Espinosa, Cooper & Barz, 1982).

The cubic lattice parameters as obtained from X-ray powder diffraction (Guinier camera, Fe $K\alpha$ radiation, Si as an internal standard) were $a_{II'}$ = 13·772 (2) and $a_{II'}$ = 13·775 (6) Å for the M = Tb, M' = Rh and M = Dy, M' = Os compounds, respectively; they are in good agreement with those reported by Espinosa, Cooper & Barz (1982).

The X-ray investigations were focused on the M = Tb, M' = Rh compound. Long-exposure precession photographs (over 200 h) were taken with a precession camera equipped with Mo $K\alpha$ radiation. The intensity measurements were carried out with a small crystal ground into a sphere (r = 0·012 cm, μr = 1·95), mounted on a four-circle Philips diffractometer (graphite monochromator, Ag $K\alpha$ radiation). The integrated intensities were measured by the ω-scan technique with a variable scan width given by $\delta\theta = 1{\cdot}50 + 0{\cdot}20 \tan\theta$, and a variable speed according to the intensity. In the θ = 3–30° range, 15 504 reflections were measured. The integrated intensities were first averaged in the $m3m$ point group and then converted into structure factors by applying the Lorentz, polarization and absorption corrections. This led to 448 independent reflections. In order to decrease the extinction effects, reflections with $\sin\theta/\lambda < 0{\cdot}40$ Å^{-1} were excluded from the refinements. It was also decided to exclude the weak reflections corresponding to $F^2 < 10\sigma(F^2)$. Since we are dealing with disordered crystals and the aim is to obtain the average structure, it is not unreasonable to use such drastic conditions. The subsequent refinements (on F) were based on 303 independent reflections and the weighting scheme $w = 1/\sigma(F^2)$ was used throughout the refinements.

As stated above, the precession photographs confirmed that the phase II′ lattice is closely related to that of phase II. The indexing led to an f.c.c. space group; however, there were intermittent diffuse-scattering streaks parallel to the {100} directions of the cubic cell ($a_{II'} \times a_{II'} \times a_{II'}$). It may be seen from Fig. 1 that they form intermittent squares centered around the cubic lattice nodes. By comparing the corresponding lattice planes of phase II and II′, schematically

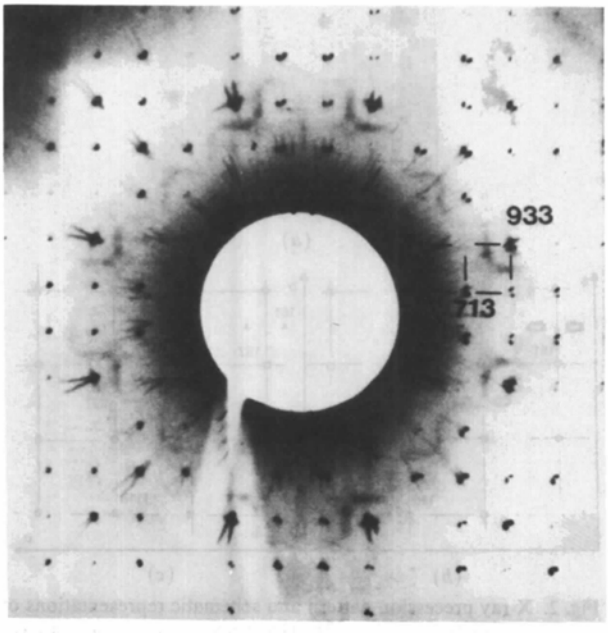

Fig. 1. X-ray precession pattern of the ($hk3$) plane for $(Sn_{1-x}Tb_x)Tb_4Rh_6Sn_{18}$.

drawn in Fig. 2, one sees that the streaks forming the squares correspond to the superstructure spots which are responsible for the doubling of the c axis of phase II.

In a previous paper (Hodeau, Marezio & Remeika, 1984) the presence of such diffuse streaks was interpreted qualitatively as due to a disorder between the $M(2)$ and Sn(2) atoms. It was also surmised that the structure was built up of phase II microdomains differentiated by the interchange of the $M(2)$ sublattice with that of Sn(2), while the rest of the structure remained unchanged. The refinement of the average structure corroborated this latter assumption. We report herein the main features of the refinement results. More details are given elsewhere (Hodeau, 1984).

The determination of the M = Tb, M' = Rh compound structure was first attempted in the $Fm3m$ space group. The cubic symmetry was simulated by the superposition of three tetragonal phase II cells related by the threefold axis $[11\frac{1}{2}]_{II}$ and a $(00\frac{1}{2})$ translation of the origin. In this simulation it is assumed that the domains are small enough so that the total calculated structure factor is the sum of the structure factors of each individual. It should be noted that in a given cell only half of the Sn(2) and $M(2)$ $Fm3m$ 32f positions are occupied. Moreover, if the $(x'x'x')$ position is occupied by one of the two atoms, the corresponding $(x''x''x'')$ position must be empty. In this case the $Fm3m$ atomic positions are used to calculate the structure factors. Each atom was given an isotropic thermal parameter. That of Sn(4) was very large because the position of this atom is poorly described in the $Fm3m$ space group. Although strong correlations existed among the refined parameters convergence was attained. The final R and wR factors were 0·082 and 0·076, respectively. The final positional and thermal parameters are reported in Table 1. These results clearly showed the close relationship between the structures of phases II and II′. Another attempt to refine the structure of phase II′ was made by assuming the $I4_1/acd$ space group. In this case the cubic reflections were considered to contain the contributions of three equal twins, *i.e.* it was assumed that the individual's size was large enough so that the total intensity was the sum of the intensities of each individual. The intensities could be thus added incoherently. By using the 303 independent reflections, the refinement yielded $R = 0{\cdot}074$ and $wR = 0{\cdot}077$. These results show that the atomic positions of a twinned phase II give a correct description of the phase II′ structure. The thermal parameters were given the corresponding values of the M = Er, M' = Rh compound (Hodeau, Marezio & Remeika, 1984) and kept fixed. The occupation factor of the Sn(4) site was also varied. Its value [0·80 (6)] proved that this site is occupied. The final positional parameters are reported in Table 2.

It can be concluded from these refinements that phase II and phase II′ compounds have the same chemical formula, namely $(Sn_{1-x}M_x)M_4M'_6Sn_{18}$; they also show to what extent the respective structures are related to each other. As far as the disorder of the $[M(2)_4Sn(2)_4]$ sublattice was concerned, no model could be proposed by considering the refinement results only. Diffuse scattering studies were thus undertaken by electron diffraction.

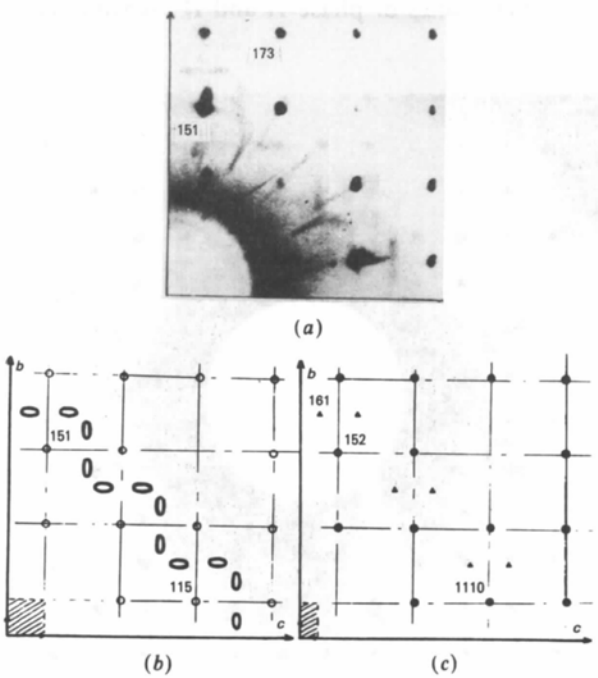

Fig. 2. X-ray precession pattern and schematic representations of the (1kl) plane for $(Sn_{1-x}Tb_x)Tb_4Rh_6Sn_{18}$: (*a*) X-ray pattern; (*b*) schematic phase II′ representation; (*c*) schematic representation of untwinned phase II.

Electron diffraction studies

Electron diffraction studies were carried out on the M = Dy, M' = Os compound by using a Philips EM 400T microscope operating at 120 kV. A double-tilting goniometer stage was used to reach different planes in reciprocal space with the same sample. Single crystals were first crushed and then transferred to holey carbon-coated copper grids.

The electron diffraction patterns revealed the same type of diffuse streaks as previously observed for the M = Tb, M' = Rh compound. However, the streaks observed in the electron diffraction photographs were continuous. A series of tilting experiments around different crystallographic axes were carried out. Examples are given in Figs. 3(*a*), 4(*a*), 5(*a*) and 6(*a*). The diffuse reciprocal lattice was reconstructed by inserting a schematic representation of each pattern in the cubic reciprocal lattice $(a_{II'} \times a_{II'} \times a_{II'})$, see Figs. 3(*b*), 4(*b*), 5(*b*), and 6(*b*). It may be seen in

Table 1. *Positional and thermal parameters for* $(Sn_{1-x}Tb_x)Tb_4Rh_6Sn_{18}$ *with the* $Fm3m$ *space group and the* $a_{II'} \times a_{II'} \times a_{II'}$ *unit cell*

		x	y	z	B
$M(1)$*	4(*b*)	1/2	1/2	1/2	0·92 (6)
Tb(2)	32(*f*)(×0·5)	0·1371 (3)	0·1371	0·1371	0·63 (3)
Sn(2)	32(*f*)(×0·5)	0·0876 (5)	0·0876	0·0876	0·78 (4)
Sn(3)	96(*k*)(×0·5)	0·1745 (2)	0·1745	0·5131 (2)	0·74 (2)
Sn(4)	8(*c*)	1/4	1/4	1/4	>30
Rh	24(*e*)	0·2447 (2)	0	0	0·47 (2)

* $M(1) = Sn(1)_{1-x}Tb(1)_x$; $x = 0·6$ (1).

Table 2. *Positional parameters for* $(Sn_{1-x}Tb_x)Tb_4Rh_6Sn_{18}$ *with the* $I4_1/acd$ *space group and the* $a_{II'} \times a_{II'} \times 2a_{II'}$ *unit cell*

		x	y	z
$M(1)$*	8(*b*)	0·0	0·0	1/4
Tb(2)	32(*g*)	0·1380 (4)	0·1364 (4)	−0·0685 (1)
Sn(2)	32(*g*)	0·0850 (7)	0·0898 (4)	0·0438 (1)
$Sn(3)_1$	16(*f*)	0·179 (2)	0·179	1/4
$Sn(3)_2$	16(*f*)	0·331 (2)	0·331	1/4
$Sn(3)_3$	32(*g*)	0·3231 (5)	0·0115 (8)	0·0870 (1)
$Sn(3)_4$	32(*g*)	−0·005 (2)	0·3271 (5)	0·0875 (1)
Sn(4)†	16(*e*)	1/4	0·205	1/8
Rh_1	16(*d*)	0·0	0·0	0·01225 (1)
Rh_2	32(*g*)	0·245	0·002	0·000

* $M(1) = Sn(1)_{1-x}Tb(1)_x$; $x = 1·0$ (1).
† Occupation factor = 0·80 (6).

Fig. 7(*a*) that the diffuse streaks are lines parallel to the {100} cubic directions; thus they are directed along the $a^*_{II'}$ axes, going through the F-centering-forbidden nodes. These diffuse lines are related by the cubic threefold axis $[111]_{II'}$ (Figs. 7*b*,*c*,*d*).

Discussion

As pointed out by Hodeau, Marezio & Remeika (1984), the sublattice responsible for the disorder is that of the $M(2)_4Sn(2)_4$ atoms. The $M(2)$ atoms form distorted tetrahedra arranged as an f.c.c. lattice and each tetrahedral face is capped with an Sn(2) atom. As these atoms are also arranged as distorted tetrahedra, the $M(2)_4Sn(2)_4$ sublattice consists of an f.c.c. lattice of 'interpenetrated tetrahedra' (Fig. 8). These interpenetrated tetrahedra can have two orientations related by a 90° rotation around a four-fold axis (Fig. 8). One goes from one orientation to the other by substituting $M(2)$ atoms with Sn(2) atoms. Hereafter, an interpenetrated $[M(2)_4Sn(2)_4]$

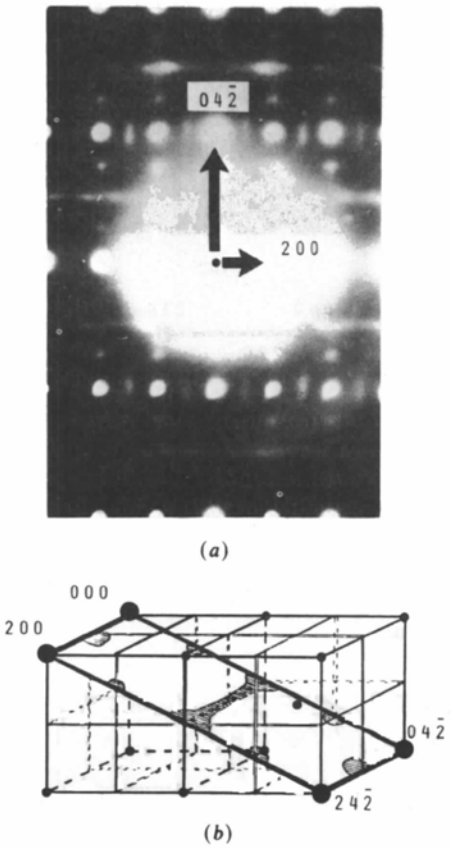

Fig. 3. (*a*) Electron diffraction pattern perpendicular to the [012] zone axis for $(Sn_{1-x}Dy_x)Dy_4Os_6Sn_{18}$. (*b*) Schematic representation.

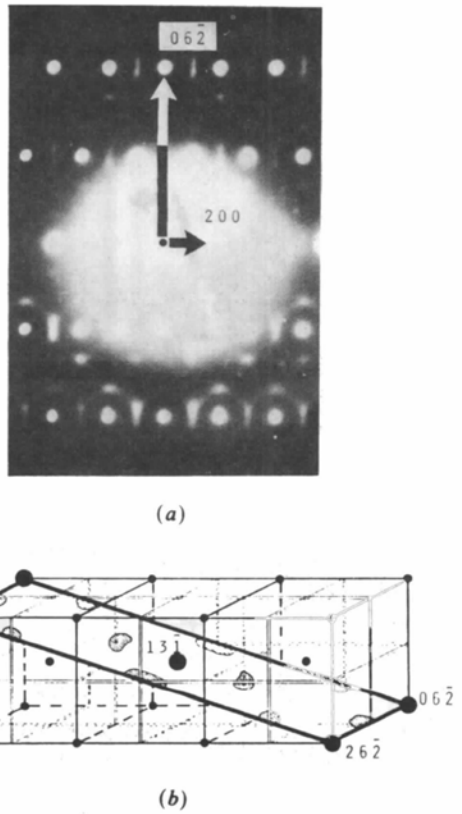

Fig. 4. (*a*) Electron diffraction pattern perpendicular to the [013] zone axis for $(Sn_{1-x}Dy_x)Dy_4Os_6Sn_{18}$. (*b*) Schematic representation.

tetrahedron will be called a 'block' and their two orientations are called *A*- and *B*-type blocks, respectively. The long-range order existing in phase II may be described as an ordered stacking along the [001] direction of equivalent planes, each consisting of a *B*-centered square lattice of *A* blocks. Each plane is related to the next by a 4_1 axis located at the $(\frac{1}{4}\frac{1}{4}0)$ position. Such a lattice is shown in Fig. 9. It is worth noting that such an arrangement is analogous to that of Fe and Li atoms in the tetragonal ordered Q_1 phase of $LiFeO_2$ (Barblan, Brandenberger & Niggli, 1944).

It can be demonstrated that uncorrelated planes along the [001] direction, as far as the relative *A* and *B* positions are concerned, give rise to diffuse streaks as shown in Fig. 7(*b*). If the structure is twinned by a threefold $[111]_{II'}$ pseudo-axis, the stacking disorder in the *A*,*B* lattice occurs along the three {100} pseudo-cubic directions and the (*b*), (*c*), (*d*) lattices of Fig. 7 are obtained for each individual, respectively. By electron diffraction the lattice corresponding to Fig. 7(*a*) was observed for phase II′. This means that the domains are smaller than the selected area and therefore the disorder of phase II′ may be regarded as a microtwinned stacking disorder of (*A*,*B*) square planes. This disorder is schematized in Fig. 10.

A different approach has been developed to explain the diffuse intensity distribution in the reciprocal lattice of a disordered crystal. Introduced by Brunel, de Bergevin & Gondrand (1972), extended by Sauvage & Parthé (1974), and improved by de Ridder, Van Tendeloo, Van Dyck & Amelinckx (1976) and de Ridder, Van Dyck, Van Tendeloo & Amelinckx (1977), this method, based on the concept of perfect local order, requires that the structure contains atom clusters (tetrahedra, octahedra, cubes *etc.*) which have the same composition as the crystal and that the atoms contributing to the disorder form a Bravais lattice.

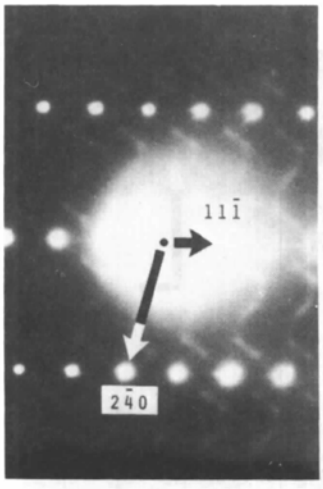

(*a*)

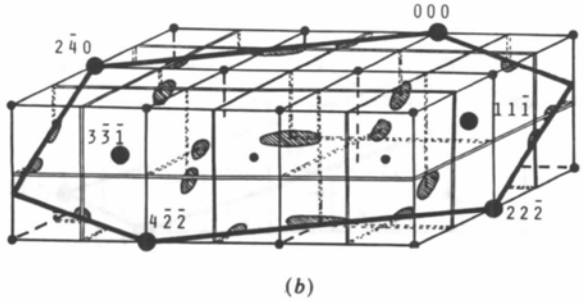

(*b*)

Fig. 5. (*a*) Electron diffraction pattern perpendicular to the [213] zone axis for $(Sn_{1-x}Dy_x)Dy_4Os_6Sn_{18}$. (*b*) Schematic representation.

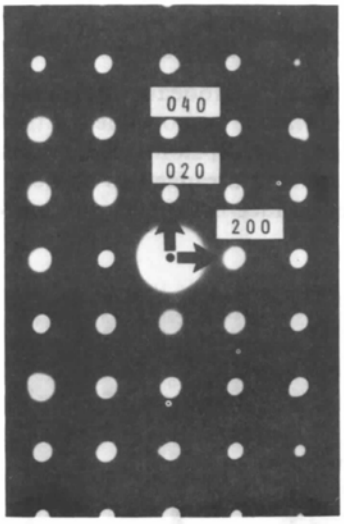

(*a*)

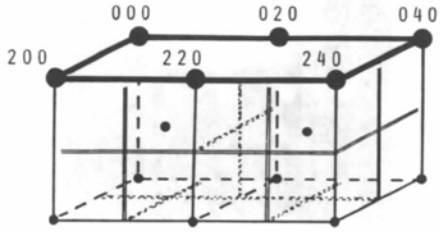

(*b*)

Fig. 6. (*a*) Electron diffraction pattern perpendicular to the [001] zone axis for $(Sn_{1-x}Dy_x)Dy_4Os_6Sn_{18}$. (*b*) Schematic representation.

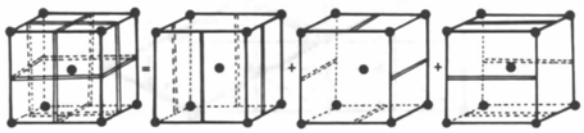

(*a*) (*b*) (*c*) (*d*)

Fig. 7. (*a*) Schematic representation of the reciprocal lattice for phase II′. (*b*), (*c*), (*d*) Decomposition of the (*a*) lattice by a threefold $[111]_{II'}$ pseudo-axis.

Depending on the type of polyhedron, different diffuse intensity distributions have been obtained.

For a partially disordered structure, having a local order in some regions of the crystal, the scattering-power density is given by the sum of a periodical contribution $P(\mathbf{r})$ and of a disordered contribution $D(\mathbf{r})$. The average value of the latter contribution over the whole crystal is zero. In the perfect-local-order model for a given cluster we have: $\sum_{\mathbf{r}_i} D(\mathbf{r}_i + \mathbf{r}_j) = 0, \forall \mathbf{r}_j$. Each i atom forming the clusters is defined by a vector $\mathbf{r}_i$ whose origin is related to the cluster, and each cluster is defined by a vector $\mathbf{r}_j$. It follows that the average of the $D(\mathbf{r})$ function be zero for a cluster as well as for the entire crystal.

If the distribution of the atom sites in the cluster is described by an $\omega(\mathbf{r})$ function (set of Dirac peaks), we have: $\int \omega(\mathbf{r}) D(\mathbf{r}+\mathbf{r}_j)\, d\mathbf{r} = 0, \forall \mathbf{r}_j$. The Fourier transform of this convolution product is given by $\Omega(\mathbf{g}) F_D(\mathbf{g}) = 0$, $\forall \mathbf{g}$, where $\Omega(\mathbf{g}) = \mathrm{FT}[\omega(\mathbf{r})]$ and $F_D(\mathbf{g}) = \mathrm{FT}[D(\mathbf{r})]$. The diffuse amplitude $F_D(\mathbf{g})$ of the disordered contribution is zero when $\Omega(\mathbf{g}) \neq 0$ and it may have a value different from zero on the surface defined by $\Omega(\mathbf{g}) = 0$. Thus, the diffuse amplitude is not distributed randomly. One can determine the diffusion surface from the $\omega(\mathbf{r})$ function, that is from the cluster shape. If the cluster is centrosymmetrical (octahedron, cube *etc.*) the Fourier transform $\Omega(\mathbf{g})$ is real and the diffuse scattering is localized on a surface. If the cluster is not centrosymmetrical (tetrahedron, pyramid *etc.*), the Fourier transform is complex $[\Omega(\mathbf{g}) = R(\mathbf{g}) + iI(\mathbf{g}) = 0]$ and the diffuse scattering is localized on a curve at the intersection of $R(\mathbf{g}) = 0$ and $I(\mathbf{g}) = 0$.

As stated above and shown in Fig. 8 the interpenetrated $[M(2)_4\mathrm{Sn}(2)_4]$ tetrahedra form a cubic lattice of A and B blocks; each block represents one of the two possible orientations of the interpenetrated tetrahedra. The nodes of such a lattice form an f.c.c. Bravais lattice which contains tetrahedra formed by two A and two B blocks, as shown in Fig. 9. Let us suppose that each $2A-2B$ tetrahedron is a cluster which has the same composition as the crystal, and whose i sites are represented by the vectors: $\mathbf{r}_1 = \frac{1}{4}[111]$, $\mathbf{r}_2 = \frac{1}{4}[\bar{1}\bar{1}1]$, $r_3 = \frac{1}{4}[1\bar{1}\bar{1}]$, and $\mathbf{r}_4 = \frac{1}{4}[\bar{1}1\bar{1}]$. The vector origin is at the tetrahedron center and the unit

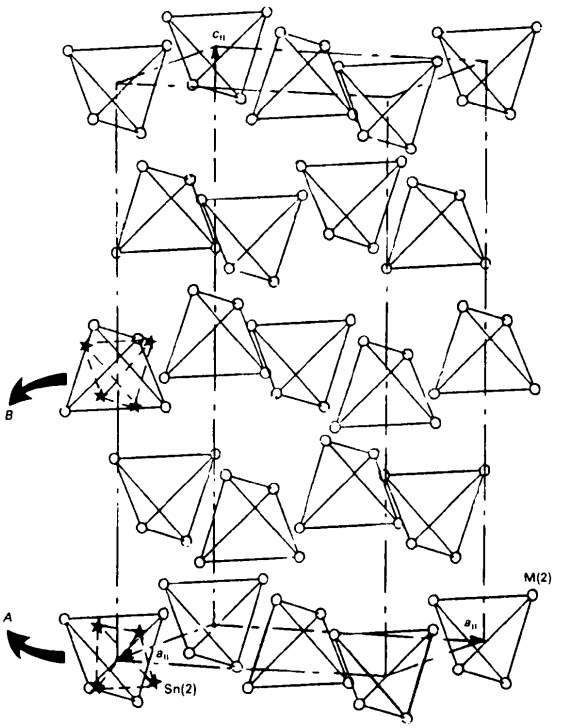

Fig. 8. The $M(2)_4\mathrm{Sn}(2)_4$ sublattice in the ordered phase II. The stars, represented only for two tetrahedra, and the open circles refer to Sn(2) and $M(2)$ atoms, respectively. Note the two possible orientations for the $M(2)_4$ tetrahedra.

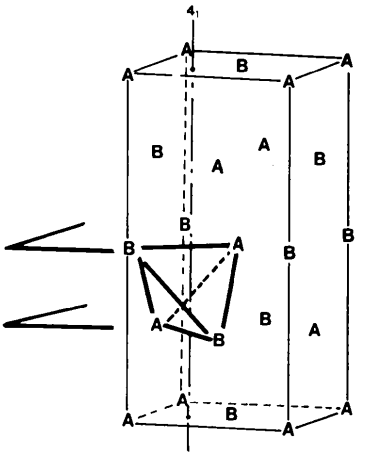

Fig. 9. The lattice of the A,B blocks in the ordered phase II. A $2A$-$2B$ tetrahedral cluster having the composition of the bulk crystal is outlined.

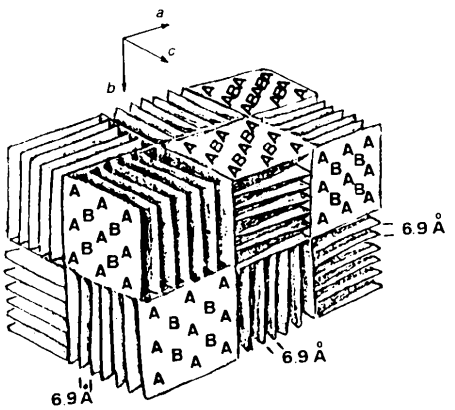

Fig. 10. Schematic representation of the stacking of uncorrelated planes along the a, b and c axes for various domains of phase II′ compounds.

cell is that of the crystal, $a_{II'} - 13{\cdot}8$ Å. The Fourier transform gives:

$$\Omega(\mathbf{g}) = 0 = \sum_{\mathbf{r}} \omega(\mathbf{r}) \exp(2\pi i \mathbf{g} \cdot \mathbf{r})$$
$$= \exp[i\pi/2(h+k+l) + \exp[i\pi/2(-h-k+l)]$$
$$+ \exp[i\pi/2(h-k-l)]$$
$$+ \exp[i\pi/2(-h+k-l)]$$
$$= \cos h\pi/2 \cos k\pi/2 \cos l\pi/2$$
$$+ i \sin h\pi/2 \sin k\pi/2 \sin l\pi/2 = 0.$$

Its solutions $h = 2m+1$, $k = 2n$; $h = 2m$, $k = 2n+1$; $h = 2m+1$, $l = 2p$; $h = 2m$, $l = 2p+1$; $k = 2n$, $l = 2p+1$; and $k = 2n+1$, $l = 2p$ indicate that the diffuse scattering is located on streaks as shown in Fig. 7(*a*), which represents the reciprocal lattice of M = Dy, M' = Os stannide. It is easy to surmise that the disorder in this compound consists in the substitution of A with B blocks. Perfect local order exists if the substitution occurs in such a way that each tetrahedral cluster is comprised of four blocks, two of each type.

This model is compatible with that based on uncorrelated planes of blocks described above. In order to define a $2A$-$2B$ tetrahedron one has always to take into consideration two planes. Whichever stacking of planes exists in the A,B lattice, any two first-neighbor A,B blocks in a given plane can always be associated with two first-neighbor A,B blocks of the plane above or below, to form a $2A$-$2B$ tetrahedron. The reversed reasoning also holds. It follows, in fact, from the above discussion that if an f.c.c. lattice is built up of $2A$-$2B$ tetrahedra, it contains a stacking of ordered (A,B) planes. A direct geometrical proof was given by Danielian (1964). As shown in Fig. 11, at the domain walls the cluster composition is not that of the crystal. It has been shown theoretically (de Ridder, Van Tendeloo, Van Dyck & Amelinckx, 1976; de Ridder, Van Dyck, Van Tendeloo & Amelinckx, 1977) that in such a case a broadening of the diffuse pattern would be obtained. We indeed observed that the diffuse streaks of the M = Dy, M' = Os stannide were qualitatively broadened. It should be pointed out that no diffuse streak was observed in the zero layer of the [001] reciprocal plane (Fig. 6*a*). Since A and B blocks may not be differentiated by projections along the [001], [100], and [010] directions, no diffuse scattering is to be expected in the zero layer of the reciprocal planes [001], [100], and [010].

In the case of the M = Tb, M' = Rh stannide we observed intermittent rather than continuous streaks. This is due to the different level of disorder existing in the two compounds. From the dimensions of the intermittent streaks it is estimated that the domains in the M = Tb, M' = Rh stannide have a correlation length of ~50 Å in one direction and ~200 Å in the other two. The first value which is of the same order of magnitude as the cell parameters corroborates qualitatively the model based on perfect local order.

Fig. 12 shows how one goes from the reciprocal lattice of ordered and untwinned phase II to that of disordered microtwinned phase II'. It is worth mentioning that experimentally we have observed reciprocal lattices such as Figs. 12(*b*), (*c*) and (*d*), but never that corresponding to an untwinned phase II.

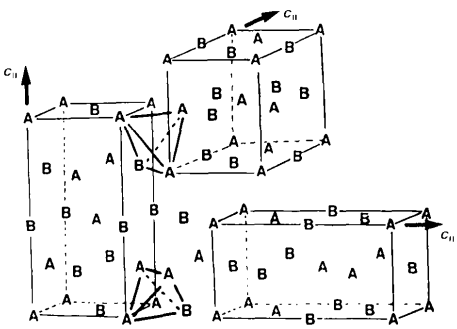

Fig. 11. Possible arrangement of the twin domains in phase II'. At the domain walls two tetrahedral clusters which do not have the bulk composition are outlined.

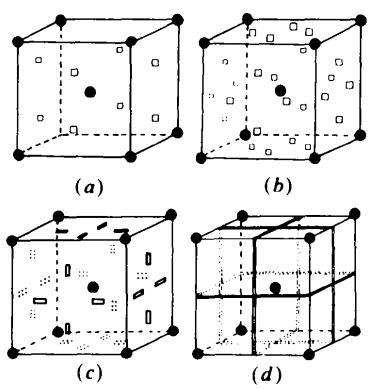

Fig. 12. Reciprocal lattice for: (*a*) ordered untwinned phase II; (*b*) ordered twinned phase II; (*c*) slightly disordered phase II'; (*d*) disordered microtwinned phase II' with perfect local order.

References

BARBLAN, F., BRANDENBERGER, E. & NIGGLI, P. (1944). *Helv. Chim. Acta*, **27**, 88-96.

BRUNEL, M., DE BERGEVIN, F. & GONDRAND, M. (1972). *J. Phys. Chem. Solids*, **33**, 1927-1942.

CHENAVAS, J., HODEAU, J. L., COLLOMB, A., MAREZIO, M., REMEIKA, J. P. & VANDENBERG, J. M. (1981). *Ternary Superconductors*, pp. 219-224. Amsterdam: North-Holland.

DANIELIAN, A. (1964). *Phys. Rev. A*, **133**, 1344-1349.

ESPINOSA, G. P., COOPER, A. S. & BARZ, H. (1982). *Mater. Res. Bull.* **17**, 963-969.

HODEAU, J. L. (1984). Thèse d'Etat, Grenoble.

HODEAU, J. L., CHENAVAS, J., MAREZIO, M. & REMEIKA, J. P. (1980). *Solid State Commun.* **36**, 839-845.

HODEAU, J. L., MAREZIO, M. & REMEIKA, J. P. (1984). *Acta Cryst.* **B40**, 26-38.

HODEAU, J. L., MAREZIO, M., REMEIKA, J. P. & CHEN, C. H. (1982). *Solid State Commun.* **42**, 97-102.

MIRAGLIA, S., HODEAU, J. L., MAREZIO, M., LAVIRON, C., GHEDIRA, M. & ESPINOSA, G. P. (1986). *J. Solid State Chem.* **63**, 358-368.

REMEIKA, J. P., ESPINOSA, G. P., COOPER, A. S., BARZ, H., ROWELL, J. M., MCWHAN, D. B., VANDENBERG, J. M., MONCTON, D. E., FISK, Z., WOOLF, L. D., HAMAKER, H. C., MAPLE, M. B., SHIRANE, G. & THOMLINSON, M. (1980). *Solid State Commun.* **34**, 923-926.

RIDDER, R. DE, VAN DYCK, D., VAN TENDELOO, G. & AMELINCKX, S. (1977). *Phys. Status Solidi A*, **40**, 669-683.

RIDDER, R. DE, VAN TENDELOO, G., VAN DYCK, D. & AMELINCKX, S. (1976). *Phys. Status Solidi A*, **38**, 663-674.

SAUVAGE, M. & PARTHÉ, E. (1974). *Acta Cryst.* A**30**, 239-246.

VANDENBERG, J. M. (1980). *Mater. Res. Bull.* **15**, 835-847.

Acta Cryst. (1987). B**43**, 83-85

Basis-Set Dependence of Theoretical Deformation Density in NO_2^-

BY TOMOAKI KIKKAWA, SHIGERU OHBA, YOSHIHIKO SAITO, SHIŃICHI KAMATA AND SUEHIRO IWATA

Department of Chemistry, Faculty of Science and Technology, Keio University, Hiyoshi, Kohoku-ku, Yokohama 223, *Japan*

(*Received* 22 *August* 1986; *accepted* 17 *September* 1986)

Abstract

Electron-density distribution of a nitrite ion was calculated by the *ab initio* molecular-orbital method using STO-3G, STO-6G, MIDI4 and MIDI4* basis sets. The N–O bonding peak, which was observed in the experimental deformation density of $LiNO_2.H_2O$, could be reproduced only by using the MIDI4* basis set. This indicates the importance of polarization functions in the study of charge distribution.

Introduction

The N–O bonding electrons of the NO_2^- ion have been observed in the experimental deformation density of $K_2Na[Co(NO_2)_6]$ (Ohba, Toriumi, Sato & Saito, 1978), $[Ni(NH_3)_4(NO_2)_2]$ (Figgis, Reynolds & Wright, 1983) and $LiNO_2.H_2O$ (Ohba, Kikkawa & Saito, 1985), whereas molecular-orbital calculations using a minimal basis set did not reproduce the N–O bonding peaks (Ohba, Kitaura, Morokuma & Saito, 1979). The discrepancy seemed to be due to the inaccuracy of the theoretical calculations. The flexibility of the basis set affects the deformation density significantly (Feil, 1985). Thus, the basis-set dependence of the deformation density in NO_2^- has been examined to resolve this problem.

Theoretical calculations

The N–O bond length and the O–N–O bond angle were set to 1·252 Å and 114·7°, which are the mean values of neutron studies on $NaNO_2$ (Kay & Frazer, 1961), $Ba(NO_2)_2.H_2O$ (Kvick, Liminga & Abrahams, 1982) and $Sr(NO_2)_2.H_2O$ (Lundgren, Kvick, Liminga & Abrahams, 1985) at room temperature. Single-determinant closed-shell *ab initio* SCF calculations were performed with the program system *MOLYX* (Kamata & Iwata, 1987) on the VAX 11/750 computer of this department, using STO-3G, STO-6G, MIDI4 and MIDI4* basis sets. The MIDI4 basis set consists of three *s*- and two *p*-type contracted Gaussian functions for first-row atoms and two *s*-type functions for hydrogen. For the MIDI4* basis set, one group of *d*-type polarization function was added for first-row atoms and one group of *p*-type function for hydrogen (Tatewaki & Huzinaga, 1980). The basis-set dependence was also examined for related ions and molecules for comparison: NO_3^- with the N–O bond length 1·25 Å from the neutron study of $LiNO_3.3H_2O$ (Hermansson, Thomas & Olovsson, 1980); $HCOO^-$ with the C–O and C–H bond lengths 1·25 and 1·09 Å respectively and the O–C–O bond angle 125·5° from the neutron studies of $LiHCOO.H_2O$ (Tellgren, Ramanujam & Liminga, 1974) and NaHCOO (Fuess, Bats, Dannöhl, Meyer & Schweig, 1982); C_2H_6 in the staggered conformation with the C–C and C–H bond lengths 1·541 and 1·091 Å respectively; and HNO_2 assuming that the geometry of the NO_2 group is the same as that of NO_2^- with the N–H bond length 1·06 Å.

Discussion

The deformation density on the NO_2 plane is shown in Fig. 1. The minimal basis sets, STO-3G and STO-6G, give almost the same features and do not present the N–O bonding peak observed experimentally. The double-ζ basis set, MIDI4, also does not produce the N–O bonding peak. The same situation holds for the 4-31G basis set (Ritchie, 1985). The MIDI4* basis

0108-7681/87/010083-03$01.50